iScience, Volume *27*

Supplemental information

Auxin response factor 10 insensitive to miR160regulation induces apospory-like phenotypes in *Arabidopsis*

Silvina Pessino, Mara Cucinotta, Carolina Colono, Elena Costantini, Davide Perrone, Maurizio Di Marzo, Giada Callizaya Terceros, Rosanna Petrella, Chiara Mizzotti, Celeste Azzaro, Maricel Podio, Gianpiero Marconi, Emidio Albertini, Hugh Dickinson, Lucia Colombo, and Marta A. Mendes

SUPPLEMENTARY FIGURES

Figure S1

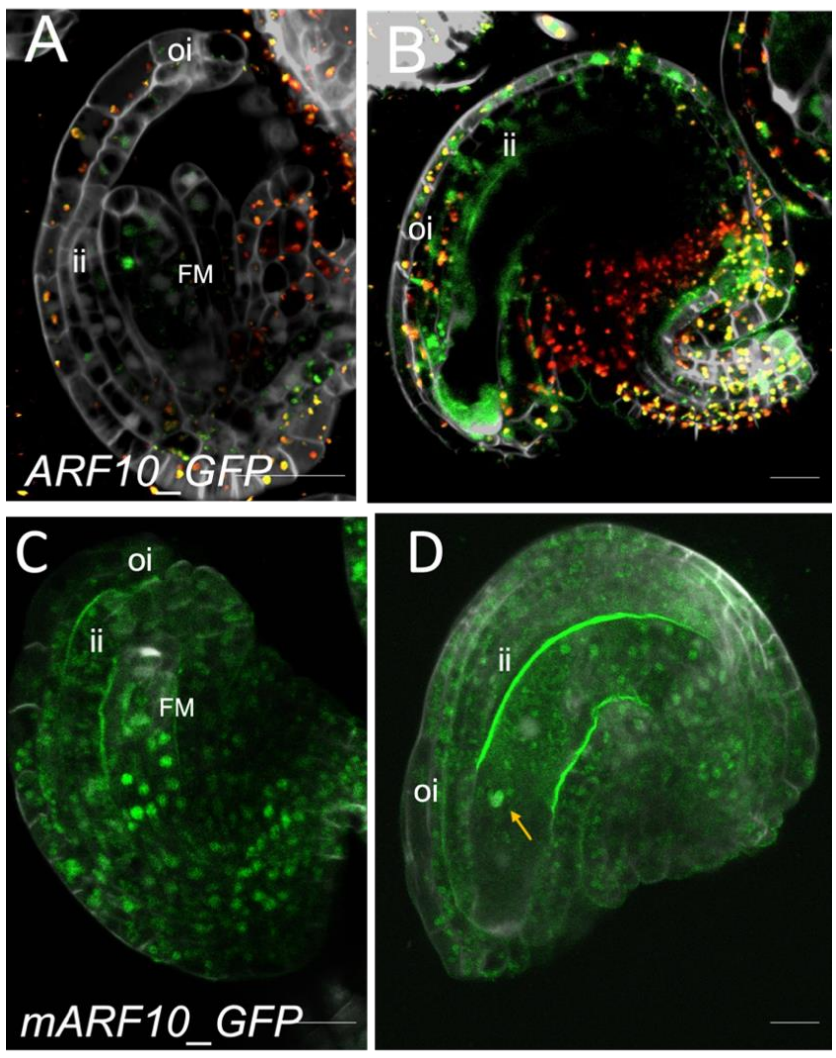

Figure S1. *ARF10_GFP* and *mARF10_GFP* expression during ovule development. (A-B) *ARF10_GFP* expression pattern during gametogenesis is detected also in the integuments. (C-D) *mARF10_GFP* expression pattern: the GFP signal is detected in all ovule cells along all different developmental stages from FG0 to FG7, even within the female germline and the female gametophyte. oi: outer integuments; ii: inner integuments; FM: functional megaspore. Scale bars: 20 μm.

Figure S2

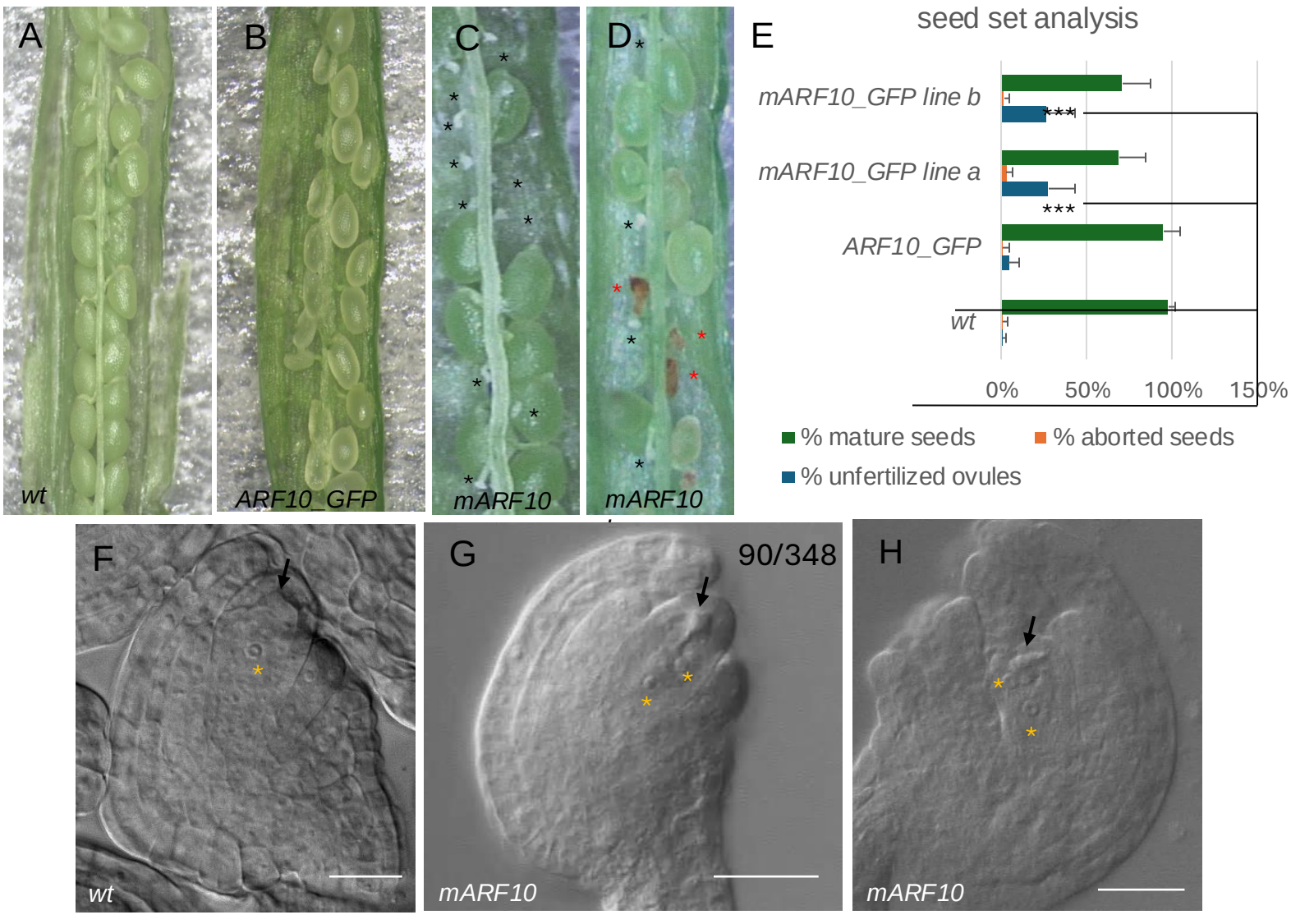

Figure S2. Fertility analysis in *mARF10* lines. (A) Stereomicroscope images of wild type; (B) *ARF10_GFP;* (C) *mARF10a* and (D) *mARF10b* siliques. Black asterisks: unfertilized ovules, red asterisks aborted seeds; (E) Graphical representation of the seed set analysis in the studied lines. Total number of ovules analysed: *mARF10a*: n=350, *mARF10b*: n=186, WT: n=243. (F-H) DIC, clearing analysis wild type (F) and *mARF10* (G-H), orange asterisks indicate functional megaspore enlarged nuclei, black arrow indicates the degenerated tetrad after meiosis. Significance evaluations between seed set of wild type and mutants were performed by the Student's t test ***P<0.01 t-student test. Scale bar: 20 μm.

Figure S3

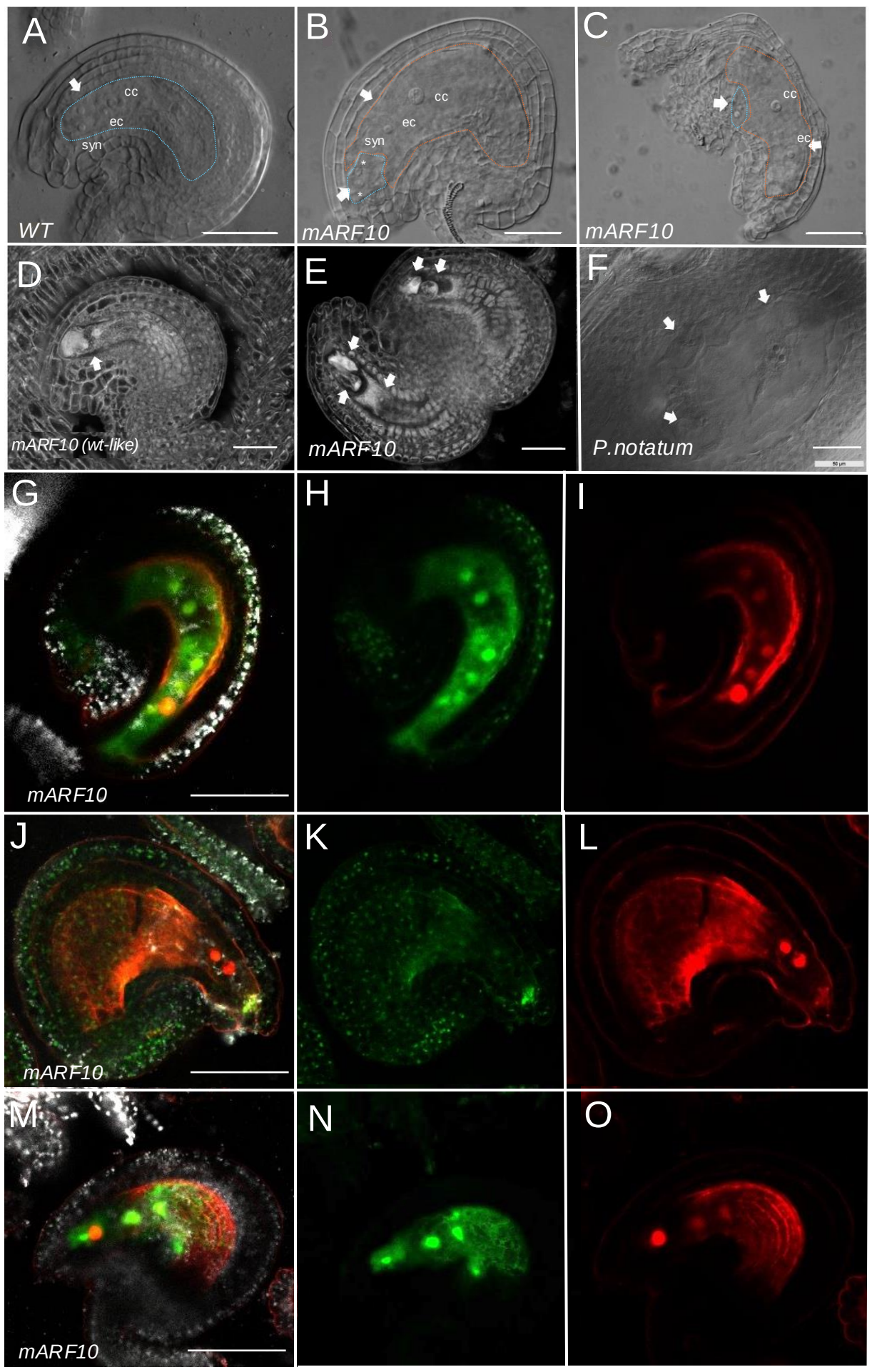

Figure S3. Embryo sacs in *mARF10* lines, cross with FGR7 (A-C) DIC, clearing microscopy. (A) A canonical meiotic embryo sac from a wild type plant. (B) Two anomalous sacs, a micropylar one with two nuclei and clear limits and a second one, larger, with one synergid, one egg cell and polar nuclei. (C) Two embryo sacs, the first one at the left, with leaf shape and clear limits; the second one larger, possible with one egg cell and polar nuclei. (D-E) Feulgen staining followed by confocal microscopy. (D) A canonical meiotic embryo sac from *mARF10*. (E) two adjacent ovules, both of them showing structures compatible with supernumerary embryo sacs. (F) For comparison, we show a *Paspalum notatum* ovule with three visible aposporous embryo sacs. White arrows indicate the embryo sacs. (G-O) *mARF10* mature ovules after hand emasculation. GFP signal corresponds to synergid cell (sc) identity, RFP signal corresponds to egg-cell (ec) identity, yellow signal (green plus red signals) corresponds to central cell (cc) identity. Left images derive from green and red combined channels. Central and right panels show green and red channels of each image, respectively, to understand the identity of the cells. (G-I): an embryo sac with multiple nuclei showing central cell identity and an egg cell still intact; (J-L): double egg-cell; (M-O): multiple embryo sacs, extra cells with displaced nuclei. Dashed lines indicate putative embryo sac limits. Scale bar: 50 μm.

Figure S4

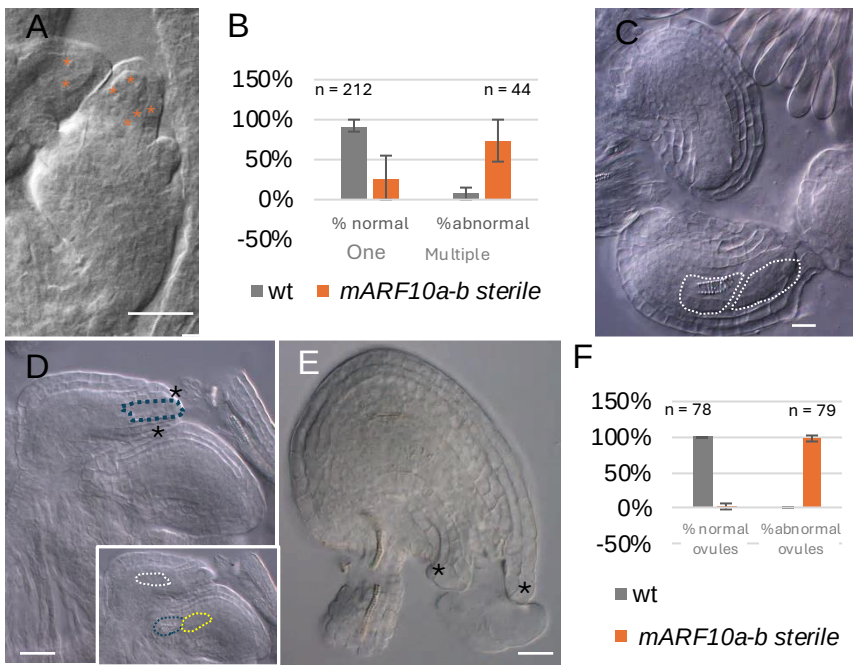

Figure S4: *mARF10* sterile phenotype characterization. (A) pre-meiotic ovule with several enlarged cells in the ovule nucellus, orange asterisks indicate the nuclei. (B) graphical representation of multiple enlarged cells identified in *mARF10* sterile lines. (C-E) post-meiotic *mARF10* ovules showing defective integument development (black asterisks), the defect is so severe that the embryo sac protrudes; putative different developing embryo sacs (dashed lines) could be detected and sometimes aborted. (F) Graphical representation of normal ovule development leading to a 7-cell embryo sac and ovules that presented abnormal development in *mARF10* sterile lines. Scale bars: 20 μm. Error bars indicate the s.e.m.

Figure S5

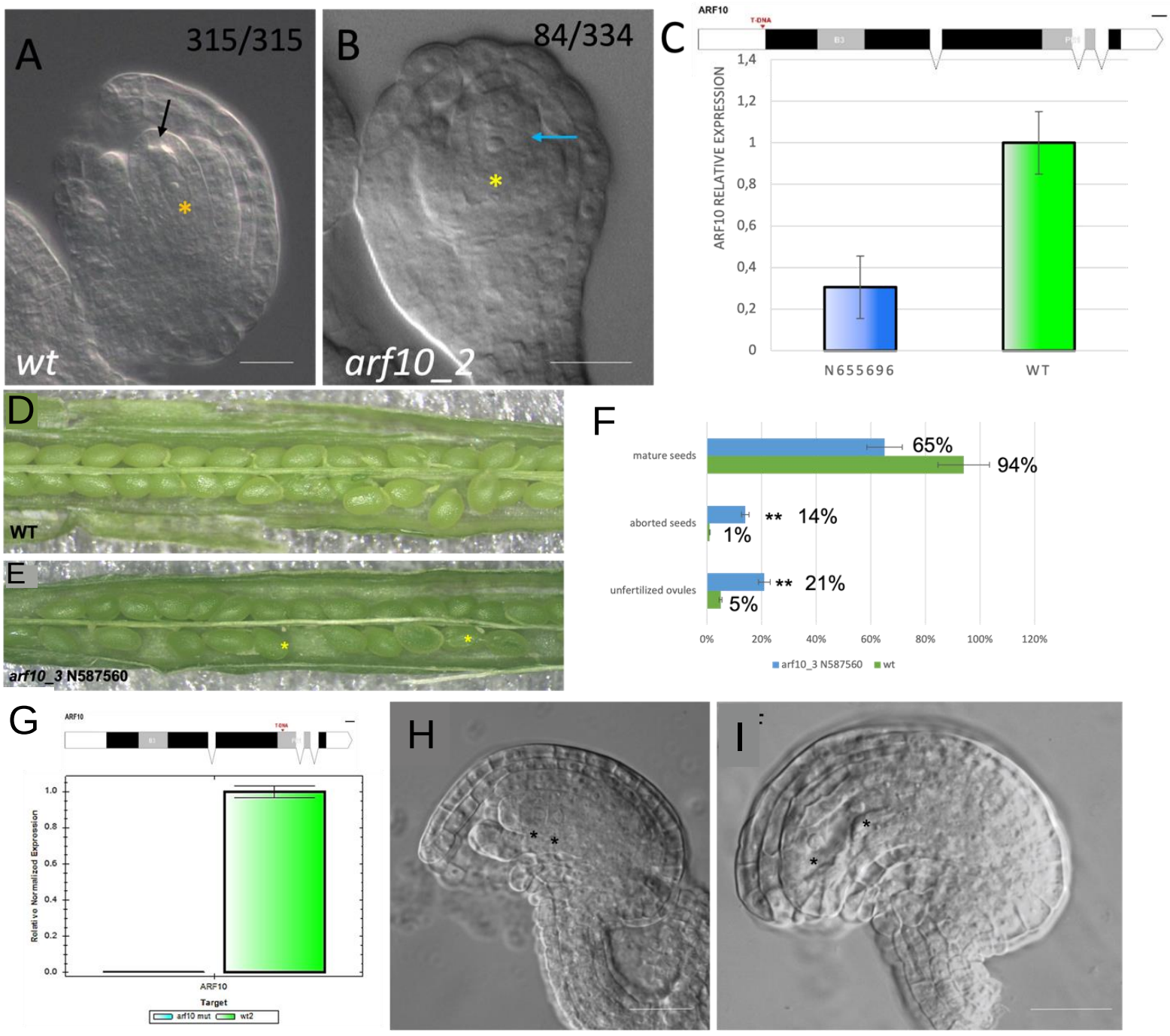

Figure S5. Reproductive characterization of *arf10_2 and arf10_3* defective mutants. DIC analysis of (A) wild type and (B) *arf10_2* mutant. In WT plants, tetrad degeneration was seen after meiosis (black arrow) (n=315 ovules) instead in *arf10_2* ovules no tetrad degeneration – a sign of late meiosis – was detected in 84 from n=334 ovules; orange asterisk indicates functional megaspore, yellow asterisk MMC after the first meiotic round, the blue arrow indicates the meiotic plate. (C) Scheme of the T-DNA insertion position and qRT-PCR results showing a decrease of *ARF10* expression in the mutant in relation to WT. (D-F) Seed set analysis in *arf10_3* when compared to wild type. Yellow asterisks show unfertilized ovules. (F) Percentage of mature seeds, aborted seeds and unfertilized ovules in WT and mutant backgrounds. Significance evaluations for the seed set between wild type and mutant were performed by the Student's t test **P<0.05 t-student test. (G) Genetic structure of the *arf10_3* (N587560) mutant allele including the T-DNA insertion position (top) and *ARF10* qPCR amplification in WT and mutant contexts (bottom). (H) delayed meiosis and (I) delayed megagametogenesis, with gametophytic arrest at 2-nuclei stage. Black asterisks indicate nuclei. Scale bars: 20 μm. For DIC imaging, significance of statistical analysis was performed using 95% Confidence Interval (CI): proportion: *arf10_3* no tetrad degeneration 62.95%; 95% CI: 0.5723 < P < 0.6833; n= 305 and *arf10_3* block in gametogenesis proportion: 30%; 95% CI: 0.2575 < P < 0.3461; n= 430).

Figure S6

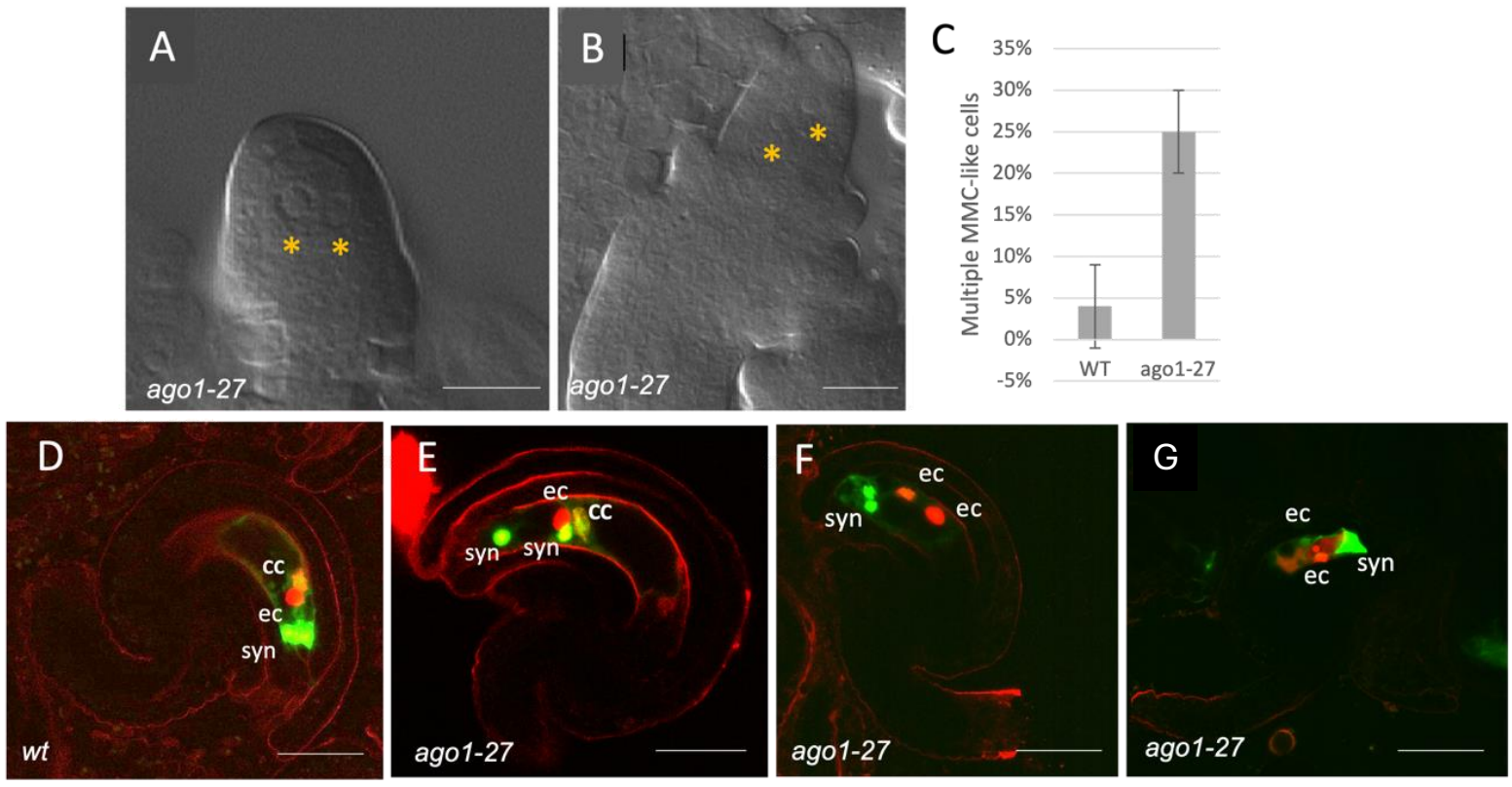

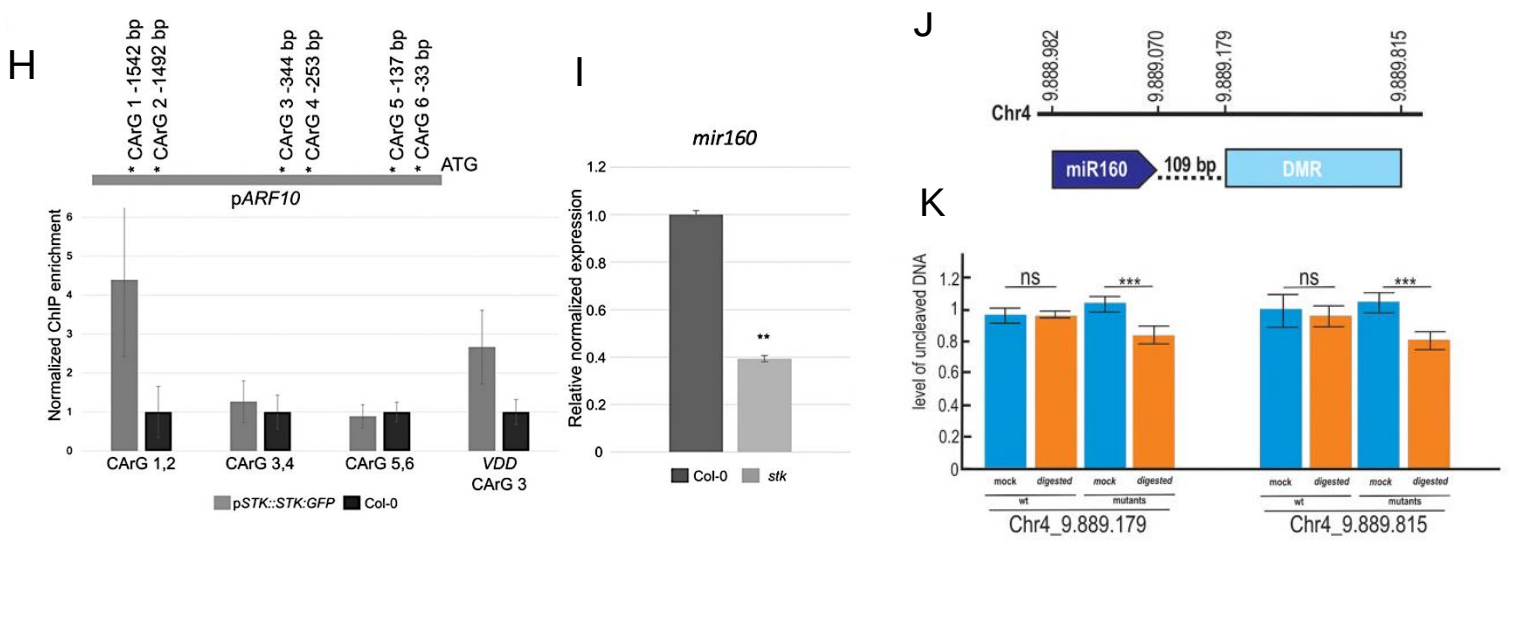

Figure S6. AGO1 and STK mediates ARF10 ovule nucellar silencing. (A-B) *ago1-27* mutant ovules
showing supernumerary enlarged cells (yellow asterisks). (C) Graphical representation of supernumerary enlarged cells percentages in wt and *ago1-27*. (D-J) FGR7.0 signal in an *ago1-27* background. GFP shows synergid cell identity, RFP egg cell identity and YFP the central cell.
Counting: abnormal ovules = 15 (n = 101). Scale bars: 20 μm. syn: synergid cells. ec: egg cell; cc: central cell. Error bars indicate the s.e.m. Significance evaluations between wild type and mutants were performed by the Student's t test **P<0.01; ***P<0.001 t-student test. (H) Upper part - CARG-boxes schematic representation in the 2000bp upstream *ARF10* transcription starting site; Lower part - representative ChIP experiment between p*STK::STK_GFP* and Col-0. Error bars represent the SD for three biological replicates. The normalized ChIP enrichment was calculated against data for wild type Col-0. *VERDANDI* (*VDD*) CaRG 3 was used as a positive control and data were normalized with *ACTIN11*. (I) Stem loop qPCR revealed expression of mature *mir160* is downregulated in *stk* when compared to wild type. (J-K) MCSeEd validation by quantitative methylation-sensitive PCR for the wild-type and *stk* mutant samples. Differentially Methylated Positions belonging to the mir160-CHH-DMR (Chr4_9.889.179 and Chr4_9.889.815) were tested. Blue shading, mock (no digestion, equivalent to a fully methylated DNA site); orange shading, digested DNA. Statistical analysis was performed using Student's t-test (***p < 0.01). Histograms show a representative experiment in which error bars represent the SD for three technical replicates. Three qPCR (biological replicates) were performed and generated similar results.

Figure S7

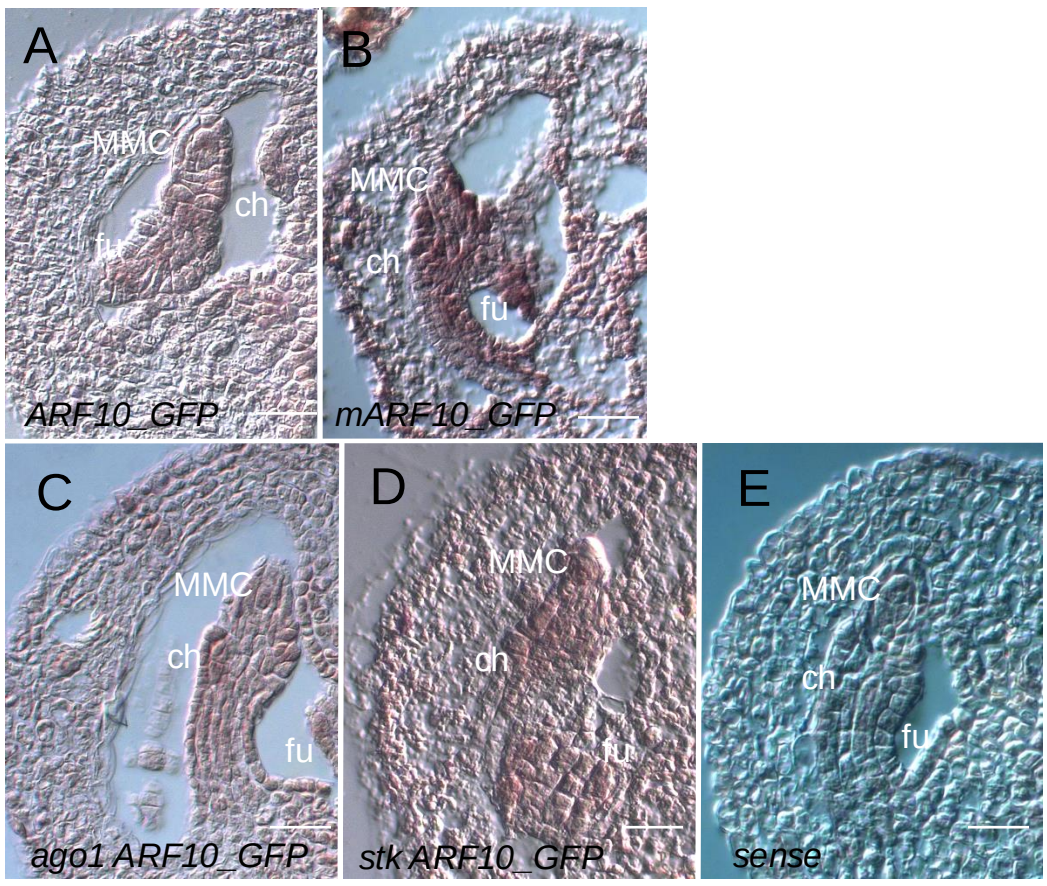

Figure S7. *In situ* RNA hybridization (A-D) antisense GFP probe. (E): sense GFP probe. (A): *ARF10_GFP* line at pre-meiosis: a faint signal is detected across the ovule; (B): *mARF10_GFP* line at pre-meiosis, the signal is stronger; (C) *ARF10_GFP* expression in *ago1*; (D): *ARF10_GFP* expression in a *stk* background; (E) no signal is detected with the sense probe. Scale bars: 10 μm.

Figure S8

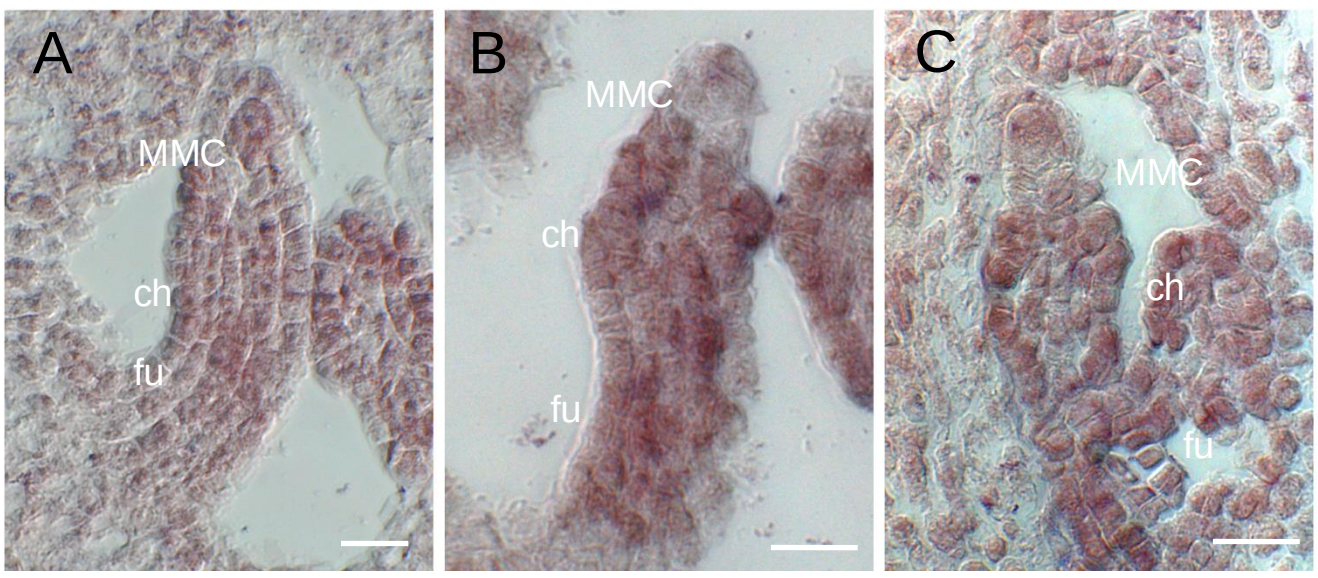

Figure S8. In situ RNA hybridization of mature miR160. (A-C): mature miR160 probe on WT (A), *stk* (B) and *ago1-27* (C). Mature miR160 expression is detected in the MMC, the chalaza (ch) and funiculus (fu) in WT and *ago1-27* ovules, but only in the chalaza and funiculus in the *stk* ovules. The signal in *stk* ovules seems to be stronger than that of the WT ones.
Scale bar: 10 μm.